HHS Public Access

Author manuscript

Int J Biochem Cell Biol. Author manuscript; available in PMC 2018 September 01.

Published in final edited form as:

Int J Biochem Cell Biol. 2017 September ; 90: 93–102. doi:10.1016/j.biocel.2017.07.005.

Dynein Binds and Stimulates Axonal Motility of the Endosome Adaptor and NEEP21 Family Member, Calcyon

Liang Shi[1], **Nagendran Muthusamy**[2], **Deanna Smith**[3,*], and **Clare Bergson**[1,*,#]

[1]Department of Pharmacology and Toxicology, Medical College of Georgia, Augusta University, Augusta, Georgia, USA

[2]Department of Neuroscience, University of North Carolina at Chapel Hill, Chapel Hill, NC USA

[3]Department of Biological Sciences, University of South Carolina, Columbia, SC, USA

Abstract

The neuron-enriched, endosomal protein Calcyon (Caly) regulates endocytosis and vesicle sorting, and is important for synaptic plasticity and brain development. In the current investigation of Caly interacting proteins in brain, the microtubule retrograde motor subunit, cytoplasmic dynein 1 heavy chain (DYNC1H), and microtubule structural proteins, α and β tubulin, were identified as Caly associated proteins by MALDI-ToF/ToF. Direct interaction of the Caly-C terminus with dynein and tubulin was further confirmed in in vitro studies. In Cos-7 cells, mCherry-Caly moved along the microtubule network in organelles largely labeled by the late endosome marker Rab7. Expression of the dynein inhibitor CC1, produced striking alterations in Caly distribution, consistent with retrograde motors playing a prominent role in Caly localization and movement. In axons of cultured adult rat sensory neurons, Caly-positive organelles co-localized with dynein intermediate chain (DYNC1I1-isoform IC-1B) and the dynein regulator, lissencephaly 1 (LIS1), both of which co-precipitated from brain with the Caly C-terminus. Manipulation of dynein function in axons altered the motile properties of Caly indicating that Caly vesicles utilize the retrograde motor. Altogether, the current evidence for association with dynein motors raises the possibility that the endocytic and cargo sorting functions of Caly in neurons could be regulated by interaction with the microtubule transport system.

Keywords

Brain; Schizophrenia; Endocytosis; Lysosome; Clathrin; Adaptor protein; AP-1; AP-2; AP-3; Tubulin

[#]Correspondence should be addressed to C.B., Department of Pharmacology and Toxicology, CB-3621, Augusta University,1459 Laney Walker Blvd, Augusta, GA 30912-2300; Office: 706-721-1926; Fax: 706-721-2345 (cbergson@augusta.edu).
[*]These authors contributed equally to the manuscript.

Introduction

The mammalian specific gene product Calcyon (Caly) belongs to the NEEP21/Caly/P19 family which is important for the endosomal sorting of proteins that regulate brain development and function (Hirling, 2009; Lasiecka and Winckler, 2011; Muthusamy et al., 2014, 2009; Yap and Winckler, 2012). Cargos sorted by NEEP21 and Caly range from GPCRs to ligand gated ion channels, and also include proteins such as neuregulin 1 and amyloid precursor protein which are prominent candidate genes in schizophrenia and Alzheimer's Disease (Muthusamy et al., 2014; Norstrom et al., 2010; Yin et al., 2014). Manipulations that increase or eliminate NEEP21 or Caly expression result in ectopic cargo localization, as well as impaired synaptic plasticity and cognitive behavior (Alberi et al., 2005; Davidson et al., 2009; Debaigt et al., 2004; Vazdarjanova et al., 2011; Yap et al., 2008). When expression of NEEP21 is knocked down, GPCRs that are typically sorted to degradative pathways undergo recycling instead (Debaigt et al., 2004). When Caly is upregulated, AMPA receptor subunits that are normally recycled to synapses, are instead degraded (Vazdarjanova et al., 2011). In contrast, levels of pre-synaptic cargoes like the zinc transporter 3 are reduced in axon terminals of Caly knockout mice (Muthusamy et al., 2012). As NEEP21 and Caly are implicated in pathological mechanisms for diseases including schizophrenia and Alzheimer's disease, it is important to obtain more detailed information about how they function in brain.

Several lines of evidence suggest that NEEP21 and Caly perform distinct endocytic and recycling functions via direct interactions with the vesicle trafficking and synaptic scaffolding machinery (Muthusamy et al., 2014). Caly interacts with μ subunits of heterotetrameric adaptor protein complexes AP-1, AP-2 and AP-3, as well as clathrin light chain (CLC) and post-synaptic protein of 95 kDa (PSD95) (Ha et al., 2012; Muthusamy et al., 2012; Xiao et al., 2006). Patch clamp peptide perfusion studies indicate that interaction with AP-2 and CLC is central to the mechanism by which Caly regulates AMPA-receptor internalization and long-term synaptic depression (LTD) (Davidson et al., 2009). In contrast, synaptic protein fractionation studies indicate that interaction with AP-3 likely underlies the role of Caly in sorting cargo proteins to axon terminals.

A goal of the present study was to obtain a framework for understanding these diverse endosomal trafficking functions by identifying other proteins that associate with Caly in brain. To that end, we conducted a proteomic investigation of brain proteins that co-purify with GST fusion protein linked to the Caly C-terminus. Among the proteins showing greatest enrichment in GST pull-down experiments were the heavy chain of cytoplasmic dynein 1 (DYNC1H) and α/β tubulin. Tubulin is the basic structural unit for microtubule cytoskeleton, whereas DYNC1H is the catalytic, force-generating subunit of the cytoplasmic dynein motor complex. Cytoplasmic dynein is the primary motor for moving cellular components, including membrane bound organelles, retrogradely towards the cell body (Maday et al., 2014). Both interactions appear to be direct as the Caly C-terminus bound selectively to intermediate chain (IC) subunits of the dynein motor complex, as well as to fractions of tubulin isolated from brain. Motility studies in Cos-7 cells revealed Caly positive organelles moved in a dynein-dependent fashion along microtubules mostly in Rab7 positive endosomes. In dorsal root ganglion (DRG) axons, Caly moved in DIC and Lis1 positive

organelles, at rates determined by DIC and Lis1 expression. Altogether, these data indicate that Caly and dynein exist in a complex in brain, and that in axons, Caly-positive organelle movement is dynein-dependent.

Materials and Methods

Preparation of brain homogenates for GST pull-down

Freshly dissected forebrains from wild-type (WT) c57bl/6 mice were homogenized in eight volumes of homogenization buffer (10mM HEPES, pH 7.4 containing 320 mM sucrose) containing protease inhibitors (Roche). Cytosolic fractions were prepared by ultracentrifugation and then pre-cleared with glutathione resin (Amersham Biosciences) added at a 1:10 ratio.

GST Pull-down

Pull-down experiments were performed as described previously (Muthusamy et al 2012). Briefly, equal amounts of glutathione-S-transferase (GST) and a fusion protein consisting of GST fused to residues 104 to 217 of human Caly (NCBI accession no. NP_056537) (GST-Caly-C) were bound to glutathione resin and blocked. Pre-cleared cytosolic fractions were added to resins and nutated overnight at 4°C. Proteins bound to glutathione resin were eluted and resolved by 1-dimensional SDS-PAGE. Gels were fixed and immersed overnight in SYPRO ruby stain. After de-staining, bands were visualized with 260 nm light. Alternatively, brain proteins pulled-down from brain were resolved on gradient gels were transferred to polyvinylidene fluoride (PVDF) membranes, and probed with anti-DIC (sc-13524, Santa Cruz), anti-Lis1 (in-house rabbit polyclonal antibody) or anti-GST (sc-459, Santa Cruz) antibodies. Similarly, purified bovine brain tubulin (5 μg) (MP Biochemicals; catalog no. 771121) or purified dynein complex (0.2 μg) (generous gift of Steve King, University of Central Florida) were used to detect direct binding of GST-Caly. Eluted proteins were transferred to PVDF membrane and incubated with anti-β-tubulin (1:1000; DSHB, Iowa; catalog no. E7-a) or anti-DIC antibodies followed by HRP conjugated secondary antibodies (1:20,000) (Jackson ImmunoResearch). For overlay assays with S-tagged hCaly (93-217)(Vazdarjanova et al., 2011), highly purified dynein complex was loaded on SDS-PAGE gels, and transferred to PVDF membrane, stained by SYPRO Ruby Protein Blot Stain reagent (S11791, ThermoFisher) to reveal dynein subunits, and then probed by 0.1mg/mL S-Caly. After washing in TBST, S-Caly binding was detected with 1:2,000 S-protein HRP conjugate (69047, Novagen). Antibody binding was revealed by chemiluminescence (ECL, GE Amersham).

In-gel digestion and Protein Identification by MALDI-TOF/TOF MS

Gel slices were cut into pieces, dehydrated with acetonitrile (ACN), and digested in sequence-grade trypsin (15 μl of 12.5mg/ml) in the presence of ammonia bicarbonate (15 μl of 50 mM solution) for 12-14 hours at 37°C. Water soluble and hydrophobic peptides were combined following extraction of the latter using formic acid (FA, 5%) in 60% ACN, vacuum-dried. The dried peptide mix was reconstituted with 0.5%TFA in 50% ACN and deposited on the MALDI plate and dried prior to adding 0.5 ml of a 1:1 dilution of saturated α-cyano-4-hydroxycinnamic acid (CHCA) in 0.5%TFA in 50% ACN. Samples were

analyzed using an Applied Biosystems 4700 Proteomics Analyzer MALDI-TOF/TOF mass spectrometer, and proteins identified by combined MS+MS/MS data using the MASCOT (v2.0.00) search engine in GPS Explorer 3.6 (Applied Biosystems). A peptide m/z tolerance of 0.5 Da, a fragment ion m/z tolerance of 0.2 Da, fixed carbamidomethyl modification on the cysteine and variable methionine oxidation, and one possible missed cleavage for trypsin was used as search criteria. A confidence index (C.I.) above 95%, and a MS/MS score of 21 or greater were used as the cutoffs for positive hits.

Live Cell Imaging and Motility Analysis in Cos-7 cells

Coverslips with transfected Cos-7 cells were placed in an Attofluor® Cell Chamber (Life Technologies), immersed in pre-warmed imaging media (Hanks' balanced salt solution, supplemented with 20 mM HEPES, 1% serum, 4.5 g/l glucose), and imaged on a Zeiss LSM510 7Live confocal microscope using Plan-Apochromat 63x/1.4 oil objective. The time-lapse videos were collected at a rate of 0.5 to 2 Hz for 1 to 3 minutes. Caly positive spots were identified and tracked using the Fiji ImageJ plug-in Trackmate v. 3.5.1. Spots were detected with sub-pixel localization using the differences of Gaussian (DoG) segmenter, filtered, and linked using the Simple LAP Tracker function with the following cutoff values of distance (1.5 μm) for linking and distance (1.5 μm) and frame (2) for gap closing. Spot movement due to diffusion was eliminated by selecting tracks with total displacement greater than 2 μm. Runs were defined as spot mobility greater than 0.17 μm/sec in any segment, and pauses as movement less than 0.170 μm/sec in any segment. Spots moving less than 5 μm in 5 min were designated 'static.' Time-lapse videos were collected at a rate of 2 Hz for 5 minutes for the nocodazole, and endosomal motility studies using GFP-Rab5 (Addgene) and GFP-Rab7 (Addgene). Supplementary videos were compiled at a rate of 20 frames per second. In other experiments, transfected Cos-7 cells were fixed in 4% paraformaldehyde, and stained with EEA1 (07-1820, Millipore), Rab7 (#9367, Cell Signaling) and α-tubulin (T5168, Sigma) antibodies. Colocalization was determined using the ImageJ plugin Coloc2.

Adult rat DRG cultures

All animal work was carried out under protocols approved by the University of South Carolina Animal Care and Use Committee. Primary cultures of sensory neurons were prepared from lumbar dorsal root ganglia (DRG) of adult rats as described (Smith and Skene, 1997). Neurons were plated onto German glass coverslips (Fisher) coated with 10μg/ml poly-D-lysine (Sigma) and 10μg/ml laminin (Millipore) and maintained at 37°C, 5% CO2 in DMEM/F12 medium supplemented with 10% horse serum and 1X N1 additives.

Immunostaining of DRG neurons

For Lis1 staining, neurons were fixed in 4% paraformaldehyde 48 hours after plating, then permeabilized with 0.1% Triton X-100 for 5 min at room temperature and processed for immunofluorescence using an in-house rabbit polyclonal antibody (Pandey and Smith, 2011). For DIC and Caly (EMD Biosciences) staining, neurons were fixed in 100% ice-cold methanol for 1 min at −20°C and processed for immunofluorescence. Nuclei were visualized with Hoechst, and coverslips mounted on glass slides using ProLong Gold Antifade reagent (Invitrogen). Neurons were viewed with an Axiovert 200 (Carl Zeiss Inc.) equipped with

Plan-Neo 100X/1.30, and Plan-Apo 63X/1.40objectives, and images acquired using a charge-coupled camera (AxioCam HRm, Carl Zeiss Inc.) linked to AxioVision software (version 4.7, Carl Zeiss Inc.).

Transfection of DRG neurons

Neurons were transfected immediately after dissection using the SCN Basic Nucleofector kit for primary neurons (Amaxa Biosystems VSPI #1003) (Pandey and Smith, 2011). Complementary hairpin sequences in the pSilencer vector (Ambion) were provided by LH Tsai (MIT) and have been well characterized (Hebbar et al., 2008; Shu et al., 2004). *Lis1*: GAGTTGTGCTGATGACAAG (1,062–1,080bp), *DHC*: GAAGGTCATGAGCCAAGAA (9,753–9,771bp). Scrambled sequences were generated from these sequences, and have been shown to have no effect on expression of the relevant proteins. The full length murine Lis1, rat DYNC1I1-isoform IC-1B used for overexpression studies have been previously described (Pandey and Smith, 2011). Neurons were plated immediately following transfection and used within 2-3 days of culture for transport studies.

Fluorescence time-lapse microscopy in DRG axons

Coverslips were transferred into fresh medium containing 25 mM Hepes, pH 7.4, and 10mM Oxyrase (Oxyrase, Inc), in an air-heated microscope stage warmed to 37°C. Time-lapse microscopy was performed using a Leica confocal microscope (SP8) with a 63X objective. The zoom setting was set to sample the X/Y plane at the Nyquist rate (512×64 pixels, zoom X1.0 = 488 nm/pixel). Axon segments that were clearly linked to a specific neuronal cell body were selected for analysis. Digital images were acquired every 0.3 seconds for 2 minutes (400 frames).

Motility Analyses

Kymographs were generated from time-lapse movies using the Image J software (version 1.43u, NIH, USA) and the KymoToolBox Image J plug-in (generous gift of Frédéric Saudou, Grenoble Institute of Neuroscience, University of Joseph Fourier, France) to differentiate motile and static organelles, and to analyze motility. Average speeds and run lengths were determined for all retrograde and anterograde “motile events” greater than 5μm.

Statistical Analysis

Experimental results are presented as the average obtained in at least three independent replicates, involving analysis of 6-12 axon segments (100 μm in length) per replicate. Grouped data were compared by t-test or one-way ANOVA followed by Dunnett’s post-test using GraphPad Prism 5.

Results

Proteomic Study of Caly Interacting Proteins Isolated from Brain

We sought to identify Caly interacting proteins in brain by glutathione-S-transferase (GST) pull-down studies followed by mass spectrometry (MS). Homogenates of mouse forebrain

were incubated with GST fused to the presumptive cytoplasmic C terminal domain of human Caly (GST-Caly-C) which contains sequence motifs critical for binding to heterotetrameric adaptor μ subunits, CLC and PSD95. Alternatively, homogenates were incubated with unconjugated GST (GST only) to control for non-specific binding to the Caly fusion partner. The main criteria for picking bands were that bands should be prominent in the GST-Caly-C lane, and be either absent, or of much weaker in intensity in the GST lane. Eight bands showing evidence of 'enrichment' in the GST-Caly-C lanes were subjected to MALDI-TOF mass spectrometry (MS) (fig. 1A).

Peptide searches of the NCBI non-redundant database were conducted to identify the corresponding proteins. Candidates were further culled based on the strength of the confidence index (C.I.) score, as well as the agreement in the predicted size of the protein with the mobility of the band on SDS-PAGE. This winnowing process revealed that two of the bands with MASCOT C.I. scores over 98% corresponded to the microtubule retrograde motor, DYNC1H (arrow 1, fig. 1A) and the microtubule structural proteins, α and β tubulin (arrow 2, fig. 1A) (Table 1). Pull-down studies using purified brain tubulin and dynein complex also purified from brain indicated that the interactions are direct as both proteins co-precipitated with GST-Caly-C but not GST (fig. 1B,C). Overlay assays with purified Caly C-terminus revealed selective binding of IC when subunits of the purified dynein complex were separated by 1-D gel and transferred to PVDF (fig. 1D).

Caly binds to tubulin and dynein and moves along microtubules tracks

To verify association with microtubule proteins *in vivo*, we investigated Caly localization and movement by live imaging of Cos-7 cells transfected with green fluorescent protein (GFP)-tubulin and mCherry-tagged Caly (mCh-Caly). Caly-labeled organelles exhibited a high degree of overlap with the microtubule system, visualized as GFP-tubulin-labeled structures (fig. 2). The alignment of Caly puncta was most prominent in peri-nuclear regions encompassing the microtubule-organizing center (MTOC), but was also evident along other regions of the microtubule network (fig. 2A-F). These data are consistent with an interaction of Caly with α and β tubulin proteins *in vivo*.

Particle tracking of time-lapse images indicated that the trajectories made by Caly in Cos-7 cells were mainly linear, but frequently included sections with vectors projecting in different directions. We classified the Caly tracks as 'inward' or 'outward' based on the overall direction of particle displacement relative to the MTOC, which was used as reference for minus ends. Trajectories parallel to the edges of the cell were called 'lateral,' and tracks with similar numbers of outward and inward segments were classified as 'bi-directional.' Covering an average of 20.87 ± 3.49 μm, the bi-directional tracks were significantly longer than outward (11.29 ± 2.08 μm), inward (9.10 ± 1.58 μm) and lateral (8.31 ± 1.17 μm) tracks ($p<0.05$) (fig. 2G). While bidirectional tracks as long as 37 μm were detected, track length could be underestimated as the time series were acquired in one Z-plane, so tracks were considered terminated once particles moved out of focus. Regardless of trajectory, Caly tracks aligned well with GFP-labeled tubulin. In addition, movement of multiple particles along a single route was not common suggesting that Caly trajectories are to some extent stochastic.

Segmentation analysis of tracks longer than 2 μm indicated that Caly particles moved in bursts interrupted by pauses, which could reflect cargo unloading/loading, Caly or motor detachment from microtubules, or track switching. Pauses were characterized by particle speeds less than 0.170 μm/sec, whereas segments with higher speeds were called 'runs.' Particle velocity averaged 0.53 μm/sec for the 1169 'run' segments analyzed, and did not differ between track types (fig. 2G). Speeds greater than 2.0 μm/sec were occasionally observed for some segments (fig. 2G). Altogether, these data strongly support the hypothesis that Caly moves along microtubules *in vivo*, at speeds reported for mammalian microtubule motor proteins (Shah and Cleveland, 2002).

Cytoplasmic dynein motors are important for Caly minus end directed motility in COS-7 cells

In previous sections, we established that Caly interacts with tubulin, and we characterized the movement of Caly particles along microtubules *in vivo*. Based on the enrichment of DYNC1H in the GST-Caly-C pull-down (fig. 1), movement of Caly particles along inward-directed tracks, and their accumulation near the MTOC (fig. 2), we next investigated whether this minus-end directed motor is involved in powering movement of Caly. If the distribution of Caly were dynein dependent, inhibitors of dynein function would be expected to result in an accumulation of Caly particles at the cell periphery. To investigate this hypothesis, we took advantage of a well-established modifier of dynein function, the N-terminal coil-coil CC1 peptide of the dynactin p150 subunit, which disrupts dynein function (Burkhardt et al., 1997). GFP-CC1 expression dramatically altered Caly distribution relative to that detected with GFP-tubulin (fig. 3A). When GFP-CC1 was co-expressed, Caly was mainly detected near evaginations of the plasma membrane, and the fraction near the MTOC was greatly reduced suggesting that Caly localization is dynein dependent. Consistent with this idea, treatment with the microtubule depolymerizing agent nocodazole dramatically reduced the motility of Caly indicating that to a large extent, Caly positive vesicles move along microtubule tracks. (fig. 3B; Supplemental video 1,2). Specifically, treatment with nocodazole produced a significant increase in the percentage of static Caly particles (94.7± 2.68%) relative to untreated controls (39.88±7.25%) ($p<0.01$, n=5 per group).

To distinguish whether Caly-positive organelles correspond to endosomes, we compared mCh-Caly localization to that of the early endosome (EE) markers, EEA1 and Rab5, and to the late endosome (LE) marker, Rab7. Caly co-localized with both EEs and LEs based double labeling with EEA1 and Rab7 antibodies (fig. 3C). Pearson correlation coefficients for Caly colocalization with EEA1 or Rab7 markedly differed ($r_{EEA1}=0.29\pm0.034$, $r_{Rab7}=0.52\pm0.029$; $p<0.001$, n=9 per group) indicating greater overlap with the LE marker. To visualize Caly motility in endosomes, we imaged Cos-7 cells co-transfected with GFP tagged versions of Rab5 and Rab7. Some Caly positive organelles were also positive for GFP-Rab 5 (Supplemental video 3), although these double-labeled vesicles comprised a minority of either Rab5 or Caly positive organelles. In contrast, the distribution of mCh-Caly and GFP-Rab7 extensively overlapped, with respect to both the static and the dynamic pools of these endosomes (Supplemental video 4). The striking co-localization with GFP-Rab7 is consistent with prominent localization of Caly in LEs.

Caly co-localizes with Dynein Intermediate Chain (DIC) and Lis1 in axons

The above proteomic and functional validation studies in Cos-7 cells suggest that Caly localization depends on dynein motor functionality, so we wanted to investigate whether dynein is a determinant of Caly's localization and/or movement in neurons. We reasoned that a functional interaction between Caly and dynein could occur during retrograde axonal transport, as ultrastructural analyses of brain indicated that Caly is present at pre- as well as post-synaptic terminals (Negyessy et al., 2008; Xiao et al., 2006). Retrograde transport is readily studied in cultured adult rat sensory neurons due to the polarized orientation of microtubules in the axon-like processes extended by these cells. We first asked whether endogenous Caly particles are present and whether they co-localize with cytoplasmic dynein. In this regard, we observed that Caly immunoreactivity in axons resembled the mCh-Caly particles seen in Cos-7 cells, and that many Caly particles were immunoreactive for DIC and for the dynein regulator, Lis1 (fig. 4A,C). Transiently expressed GFP-IC-1B or GFP-Lis1 also co-localized with mCh-Caly in axons (fig. 4B,D), and tracked with moving mCh-Caly particles (fig. 4E) suggesting that these tagged versions behaved similarly to endogenous proteins. These data are consistent with the functional association of Caly and dynein motors in axons. The ability of GST-Caly but not GST to pull down of DIC and Lis1 from homogenates of mouse brain further substantiates this idea, and suggests that Caly could be part of a larger dynein motor complex (fig. 4F).

Dynein drives motility of a population of Caly vesicles in axons

We next investigated the dynein dependence of Caly movement in axons. Previously, we showed that organelle motility in DRG axons was greatly diminished when DYNC1H or Lis1 expression was reduced using RNAi, and stimulated by Lis1 overexpression (Pandey and Smith, 2011). Here we report that manipulation of DYNC1H and Lis1 levels also impact the movement of mCh-Caly particles in axons. Kymographs from 2-minute time-lapse movies of organelles moving in 100 μm axon segments were used to analyze motility (fig. 5A). Reduced expression of either DYNC1H or Lis1 significantly lowered both the percentage and number of Caly organelles moving retrogradely in individual axons ($p<0.001$) (fig. 5B, C). This was accompanied by an increase in Caly organelles that remained static for the entire recording interval. Interestingly, DYNC1H RNAi also reduced anterograde movements of Caly organelles.

In addition to whole trajectory analyses, kymographs were also used to analyze "motile events", because individual organelles can pause or change speed or direction during the 2-minute interval. Changes in the speed of motile events for the same organelle could be due to changes in motor cooperation or antagonism, or could reflect other spatial or molecular environmental factors. Change in direction is likely related to a switching between kinesin and dynein "dominance". In any case, measuring movements that occur between pauses or between speed and/or direction changes can provide a more detailed view of individual motor runs. Using this analysis of mCh-Caly motility in axons, overexpression of Lis1 and dynein IC-1B were found to increase both the average speed and run length of retrograde motile events (fig. 6A-C). Lis1 overexpression also increased anterograde speed, and both Lis1 and IC-1B overexpression increased anterograde run length (fig. 6D). Taken together, these data indicate that Caly vesicles utilize dynein motors for axonal transport.

Discussion

The vertebrate specific NEEP21/Caly/P19 gene family is highly enriched in the central nervous system, and important for endosomal sorting of cargo proteins that regulate brain development and synaptic function, and also play a role in neurodegenerative, cognitive and behavioral disorders (Muthusamy et al., 2014). Although some cargos have been identified, the overall role of the NEEP21/Caly/P19 gene family in neurons remains poorly understood. As a strategy for gaining greater insight into the function of these proteins in brain, we conducted MS analysis of brain proteins associated with Caly C-terminus. Previous studies describing the interactions of this gene family have largely identified established endosomal sorting proteins and synaptic scaffolding proteins (Muthusamy et al., 2012; Steiner et al., 2005; Xiao et al., 2006). In contrast, the protein interaction and functional studies reported here demonstrate that motor and structural components of the microtubule transport system, namely cytoplasmic dynein and α/β tubulin, are also among the proteins associated with at least one family member.

Direct interaction of both cytoplasmic dynein IC and tubulin with Caly was confirmed using highly purified proteins from brain. While dynein is the major retrograde motor, it is also involved in bi-directional transport of a number of organelles including EE and LEs, in which NEEP21/Caly/P19 proteins localize. The prominent localization of Caly in Rab7 positive endosomes reported here is consistent with interaction of Caly with dynein motors and microtubules since LEs undergo dynein-dependent retrograde transport, and Rab7 is a dynein adaptor (Bananis et al., 2004; Johansson et al., 2007).

In some cases, Caly vesicles moved bi-directionally in DRG axons and Cos-7 cells. Bidirectional movement is consistent with localization in vesicles that have dynein as well as the anterograde motor kinesin attached (Maday et al., 2014; Schuster et al., 2011). Caly was previously reported to undergo bi-directional movement in dendrites of hippocampal neurons but the involvement of motors has not been investigated (Kruusmägi et al., 2007). One model of bidirectional transport proposes that kinesin and dynein motors remain stably and simultaneously bound, and that the direction of organelle motility at any given moment is determined by relative levels of attached motor protein activity (Hendricks et al., 2010). Motor activity is regulated by a variety of mechanisms including phosphorylation, association with small GTPases, and binding of cargo adaptor proteins (Maday et al., 2014). The present observations indicate that Caly motility is dynein dependent, but whether Caly could also influence the activity of motors associated with bi-directionally moving organelles remains to be tested.

Caly motility in axons was strongly influenced by the levels of the dynein regulator Lis1, with RNAi reducing retrograde speed and run length, and over-expression increasing both indices of retrograde movement. While not identified in the initial MS proteomic analysis of Caly-C pull downs, immunoblotting suggests that Lis1 is also associated with Caly in brain. Lis1 has been shown to maintain dynein motor processivity in axons which could explain the increased run length of Caly puncta detected in Lis1-EGFP axons (Moughamian et al., 2013; Pandey and Smith, 2011; Smith et al., 2000). Lis1 also functions at plus-ends in recruiting dynein, and initiating dynein-mediated retrograde movement (Moughamian et al.,

2013), which is consistent with the increase in percent of retrograde moving Caly puncta observed in our studies. At minus ends, Lis1 facilitates the loading of dynein onto kinesin-positive organelles for transport to plus ends (Taya et al., 2007; Yamada et al., 2008). Thus, Lis1-related alterations in Caly anterograde movement could reflect an indirect 'hitchhiking' effect by virtue of the ability of Caly to bind directly to IC (Salogiannis and Reck-Peterson, 2016).

We undertook an unbiased proteomic approach to identify interacting proteins from brain. However, a limitation of our strategy is that we picked only 'enriched' bands for MS analysis. In this respect, interacting proteins would likely not be identified in our pull-down assay if they were less strongly associated under the conditions used. Indeed, other work has shown that buffer composition can impact the range of microtubule-associated proteins recovered in proteomic studies (Kozielski et al., 2010). Nevertheless, the localization, trajectory, and motility data presented here strongly argue that the interactions detected in our pull-down experiments are functional, which validates the biological relevance of the findings obtained in these studies.

Caly is the only member of the tripartite gene family that is found in axons, and here we report that Caly motility in axons is dynein-dependent. Phylogenetic studies suggest that the gene emerged late in evolution, as Caly orthologs are found only in mammals, whereas those of NEEP21 and P19 are present in bony fish (Muthusamy et al., 2009). Since axons of mammalian motor neurons can exceed a meter in length, the current findings raise the possibility that the interaction with microtubule system could represent an adaptation geared toward optimizing the functionality of the endocytic and cargo sorting machinery in the mammalian CNS. While our studies confirm that dynein regulates Caly motility in axons, it is important to note that dynein is also present in dendrites, and that DYNC1H is one of the most abundant proteins found in preparations of excitatory post-synaptic terminals (Cheng et al., 2006). Ultrastructural studies indicate that Caly is also expressed in dendrites and present in dendritic spines which are sites of excitatory input (Negyessy et al., 2008; Xiao et al., 2006). Therefore the functional interaction cytoplasmic dynein defined here in axons could also be relevant for understanding the post-synaptic functions of Caly, including its role in regulating synaptic plasticity via effects on AMPA receptor internalization (Davidson et al., 2009).

Dynein is best known in neuroscience for its role in neuronal migration and axonal transport. Mutations in the dynein motor complex in humans have been associated with neurodevelopmental abnormalities such as lissencephaly, and motor neuron diseases including amyotrophic lateral sclerosis (Hirokawa et al., 2010; Willemsen et al., 2012). However, recent work suggests that dynein could also play a role in neuropsychiatric disorders as two leading candidate genes, disrupted in schizophrenia-1 (DISC1) (Jaaro-Peled et al., 2009; Kamiya et al., 2005; Kvajo et al., 2011; Morris et al., 2003) and dystrobrevin-binding protein 1 (dysbindin-1) (Talbot et al., 2006), both encode proteins that are associated with microtubules. DISC1 interacts with dynein regulatory proteins Lis1 (Bradshaw et al., 2011), whereas dysbindin-1 is a subunit of the BLOC-1 complex that interacts with snapin which binds dynein IC (Di Pietro et al., 2006; Ghiani et al., 2010; Larimore et al., 2011; Taneichi-Kuroda et al., 2009). If dynein function is altered in neuropsychiatric disorders, the

present findings showing that Caly directly interacts with dynein IC could be linked to the increased levels of Caly mRNA and protein detected schizophrenia (Bai et al., 2004; Baracskay et al., 2006; Clinton et al., 2005; Koh et al., 2003).

In summary, our findings suggest that endosome adaptor Caly is present in a multi-protein complex in brain that includes motor, structural and regulatory components of the microtubule transport system. Given the intimate association and impact of dynein motor function on Caly distribution and movement, it is possible that this retrograde motor could exert a major influence on Caly's endocytic and vesicle sorting functions in axons and dendrites, as well as at synapses.

Supplementary Material

Refer to Web version on PubMed Central for supplementary material.

Acknowledgments

We are grateful to Dr. Kevin Pfister of U. of Virginia for the dynein plasmids, Dr. Steve King for purified dynein of U. of Central Florida, and Dr. J. L. Twiss of U. of South Carolina for his comments on a draft of the manuscript. This work was supported by the National Institutes of Health [Grant number: R01NS056314 (D.S.) and R21MH109280 (C.B.)].

References

Alberi S, Boda B, Steiner P, Nikonenko I, Hirling H, Muller D. The endosomal protein NEEP21 regulates AMPA receptor-mediated synaptic transmission and plasticity in the hippocampus. MolCell Neurosci. 2005; 29:313–319.

Bananis E, Nath S, Gordon K, Satir P, Stockert RJ, Murray JW, Wolkoff AW. Microtubule-dependent movement of late endocytic vesicles in vitro: requirements for Dynein and Kinesin. Mol Biol Cell. 2004; 15:3688–3697. DOI: 10.1091/mbc.E04-04-0278 [PubMed: 15181154]

Bradshaw NJ, Soares DC, Carlyle BC, Ogawa F, Davidson-Smith H, Christie S, Mackie S, Thomson PA, Porteous DJ, Millar JK. PKA phosphorylation of NDE1 is DISC1/PDE4 dependent and modulates its interaction with LIS1 and NDEL1. J Neurosci Off J Soc Neurosci. 2011; 31:9043–9054. DOI: 10.1523/JNEUROSCI.5410-10.2011

Burkhardt JK, Echeverri CJ, Nilsson T, Vallee RB. Overexpression of the dynamitin (p50) subunit of the dynactin complex disrupts dynein-dependent maintenance of membrane organelle distribution. J Cell Biol. 1997; 139:469–484. [PubMed: 9334349]

Cheng H-H, Liu S-H, Lee H-C, Lin Y-S, Huang Z-H, Hsu C-I, Chen Y-C, Chang Y-C. Heavy chain of cytoplasmic dynein is a major component of the postsynaptic density fraction. J Neurosci Res. 2006; 84:244–254. DOI: 10.1002/jnr.20898 [PubMed: 16721762]

Davidson HT, Xiao J, Dai R, Bergson C. Calcyon is necessary for activity-dependent AMPA receptor internalization and LTD in CA1 neurons of hippocampus. Eur J Neurosci. 2009; 29:42–54. [PubMed: 19120439]

Debaigt C, Hirling H, Steiner P, Vincent JP, Mazella J. Crucial role of neuron-enriched endosomal protein of 21 kDa in sorting between degradation and recycling of internalized G-protein-coupled receptors. J Biol Chem. 2004; 279:35687–35691. [PubMed: 15187090]

Di Pietro SM, Falcón-Pérez JM, Tenza D, Setty SRG, Marks MS, Raposo G, Dell'Angelica EC. BLOC-1 interacts with BLOC-2 and the AP-3 complex to facilitate protein trafficking on endosomes. Mol Biol Cell. 2006; 17:4027–4038. DOI: 10.1091/mbc.E06-05-0379 [PubMed: 16837549]

Ghiani CA, Starcevic M, Rodriguez-Fernandez IA, Nazarian R, Cheli VT, Chan LN, Malvar JS, de Vellis J, Sabatti C, Dell'Angelica EC. The dysbindin-containing complex (BLOC-1) in brain:

developmental regulation, interaction with SNARE proteins and role in neurite outgrowth. Mol Psychiatry. 2010; 15:115, 204–215. DOI: 10.1038/mp.2009.58 [PubMed: 19546860]

Ha CM, Park D, Han J-K, Jang J-I, Park J-Y, Hwang EM, Seok H, Chang S. Calcyon forms a novel ternary complex with dopamine D1 receptor through PSD-95 and plays a role in dopamine receptor internalization. J Biol Chem. 2012; doi: 10.1074/jbc.M112.370601

Hebbar S, Mesngon MT, Guillotte AM, Desai B, Ayala R, Smith DS. Lis1 and Ndel1 influence the timing of nuclear envelope breakdown in neural stem cells. J Cell Biol. 2008; 182:1063–1071. DOI: 10.1083/jcb.200803071 [PubMed: 18809722]

Hendricks AG, Perlson E, Ross JL, Schroeder HW, Tokito M, Holzbaur ELF. Motor Coordination Via Tug-Of-War Mechanism Drives Bidirectional Vesicle Transport. Curr Biol CB. 2010; 20:697–702. DOI: 10.1016/j.cub.2010.02.058 [PubMed: 20399099]

Hirling H. Endosomal trafficking of AMPA-type glutamate receptors. Neuroscience. 2009; 158:36–44. DOI: 10.1016/j.neuroscience.2008.02.057 [PubMed: 18406063]

Hirokawa N, Niwa S, Tanaka Y. Molecular Motors in Neurons: Transport Mechanisms and Roles in Brain Function, Development, and Disease. Neuron. 2010; 68:610–638. DOI: 10.1016/j.neuron.2010.09.039 [PubMed: 21092854]

Jaaro-Peled H, Hayashi-Takagi A, Seshadri S, Kamiya A, Brandon NJ, Sawa A. Neurodevelopmental mechanisms of schizophrenia: understanding disturbed postnatal brain maturation through neuregulin-1 –ErbB4 and DISC1. Trends Neurosci. 2009; 32:485–495. DOI: 10.1016/j.tins.2009.05.007 [PubMed: 19712980]

Johansson M, Rocha N, Zwart W, Jordens I, Janssen L, Kuijl C, Olkkonen VM, Neefjes J. Activation of endosomal dynein motors by stepwise assembly of Rab7-RILP-p150Glued, ORP1L, and the receptor betalll spectrin. J Cell Biol. 2007; 176:459–471. DOI: 10.1083/jcb.200606077 [PubMed: 17283181]

Kamiya A, Kubo K, Tomoda T, Takaki M, Youn R, Ozeki Y, Sawamura N, Park U, Kudo C, Okawa M, Ross CA, Hatten ME, Nakajima K, Sawa A. A schizophrenia-associated mutation of DISC1 perturbs cerebral cortex development. Nat Cell Biol. 2005; 7:1167–1178. DOI: 10.1038/ncb1328 [PubMed: 16299498]

Kozielski F, Riaz T, DeBonis S, Koehler CJ, Kroening M, Panse I, Strozynski M, Donaldson IM, Thiede B. Proteome analysis of microtubule-associated proteins and their interacting partners from mammalian brain. Amino Acids. 2010; doi: 10.1007/s00726-010-0649-5

Kruusmägi M, Zelenin S, Brismar H, Scott L. Intracellular dynamics of calcyon, a neuron-specific vesicular protein. Neuroreport. 2007; 18:1547–1551. DOI: 10.1097/WNR.0b013e3282f03f51 [PubMed: 17885599]

Kvajo M, McKellar H, Drew LJ, Lepagnol-Bestel A-M, Xiao L, Levy RJ, Blazeski R, Arguello PA, Lacefield CO, Mason CA, Simonneau M, O'Donnell JM, MacDermott AB, Karayiorgou M, Gogos JA. Altered axonal targeting and short-term plasticity in the hippocampus of Disc1 mutant mice. Proc Natl Acad Sci U S A. 2011; 108:E1349–1358. DOI: 10.1073/pnas.1114113108 [PubMed: 22049344]

Larimore J, Tornieri K, Ryder PV, Gokhale A, Zlatic SA, Craige B, Lee JD, Talbot K, Pare J-F, Smith Y, Faundez V. The schizophrenia susceptibility factor dysbindin and its associated complex sort cargoes from cell bodies to the synapse. Mol Biol Cell. 2011; 22:4854–4867. DOI: 10.1091/mbc.E11-07-0592 [PubMed: 21998198]

Lasiecka ZM, Winckler B. Mechanisms of polarized membrane trafficking in neurons – Focusing in on endosomes. Mol Cell Neurosci. 2011; 48:278–287. DOI: 10.1016/j.mcn.2011.06.013 [PubMed: 21762782]

Maday S, Twelvetrees AE, Moughamian AJ, Holzbaur ELF. Axonal Transport: Cargo-Specific Mechanisms of Motility and Regulation. Neuron. 2014; 84:292–309. DOI: 10.1016/j.neuron.2014.10.019 [PubMed: 25374356]

Morris JA, Kandpal G, Ma L, Austin CP. DISC1 (Disrupted-In-Schizophrenia 1) is a centrosome-associated protein that interacts with MAP1A, MIPT3, ATF4/5 and NUDEL: regulation and loss of interaction with mutation. Hum Mol Genet. 2003; 12:1591–1608. [PubMed: 12812986]

Moughamian AJ, Osborn GE, Lazarus JE, Maday S, Holzbaur ELF. Ordered recruitment of dynactin to the microtubule plus-end is required for efficient initiation of retrograde axonal transport. J Neurosci Off J Soc Neurosci. 2013; 33:13190–13203. DOI: 10.1523/JNEUROSCI.0935-13.2013

Mullin AP, Gokhale A, Larimore J, Faundez V. Cell biology of the BLOC-1 complex subunit dysbindin, a schizophrenia susceptibility gene. Mol Neurobiol. 2011; 44:53–64. DOI: 10.1007/s12035-011-8183-3 [PubMed: 21520000]

Muthusamy N, Ahmed SA, Rana BK, Navarre S, Kozlowski DJ, Liberles DA, Bergson C. Phylogenetic analysis of the NEEP21/calcyon/P19 family of endocytic proteins: evidence for functional evolution in the vertebrate CNS. J Mol Evol. 2009; 69:319–332. DOI: 10.1007/s00239-009-9273-y [PubMed: 19760447]

Muthusamy N, Chen Y-J, Yin D-M, Mei L, Bergson C. Complementary Roles of NEEP21 and Calcyon In Neuronal Vesicle Trafficking. J Neurochem. 2014; doi: 10.1111/jnc.12989

Muthusamy N, Faundez V, Bergson C. Calcyon, a mammalian specific NEEP21 family member, interacts with adaptor protein complex 3 (AP-3) and regulates targeting of AP-3 cargoes. J Neurochem. 2012; 123:60–72. DOI: 10.1111/j.1471-4159.2012.07814.x [PubMed: 22650988]

Negyessy L, Bergson C, Garab S, Simon L, Goldman-Rakic PS. Ultrastructural localization of calcyon in the primate cortico-basal ganglia-thalamocortical loop. Neurosci Lett. 2008; 440:59–62. [PubMed: 18539394]

Norstrom EM, Zhang C, Tanzi R, Sisodia SS. Identification of NEEP21 as a ß-amyloid precursor protein-interacting protein in vivo that modulates amyloidogenic processing in vitro. J Neurosci Off J Soc Neurosci. 2010; 30:15677–15685. DOI: 10.1523/JNEUROSCI.4464-10.2010

Pandey JP, Smith DS. A Cdk5-dependent switch regulates Lis1/Ndel1/dynein-driven organelle transport in adult axons. J Neurosci Off J Soc Neurosci. 2011; 31:17207–17219. DOI: 10.1523/JNEUROSCI.4108-11.2011

Salogiannis J, Reck-Peterson SL. Hitchhiking: A Non-Canonical Mode of Microtubule-Based Transport. Trends Cell Biol. 2016; doi: 10.1016/j.tcb.2016.09.005

Schuster M, Lipowsky R, Assmann M-A, Lenz P, Steinberg G. Transient binding of dynein controls bidirectional long-range motility of early endosomes. Proc Natl Acad Sci U S A. 2011; 108:3618–3623. DOI: 10.1073/pnas.1015839108 [PubMed: 21317367]

Shah JV, Cleveland DW. Slow axonal transport: fast motors in the slow lane. Curr Opin Cell Biol. 2002; 14:58–62. [PubMed: 11792545]

Shu T, Ayala R, Nguyen M-D, Xie Z, Gleeson JG, Tsai L-H. Ndel1 operates in a common pathway with LIS1 and cytoplasmic dynein to regulate cortical neuronal positioning. Neuron. 2004; 44:263–277. DOI: 10.1016/j.neuron.2004.09.030 [PubMed: 15473966]

Smith DS, Niethammer M, Ayala R, Zhou Y, Gambello MJ, Wynshaw-Boris A, Tsai LH. Regulation of cytoplasmic dynein behaviour and microtubule organization by mammalian Lis1. Nat Cell Biol. 2000; 2:767–775. DOI: 10.1038/35041000 [PubMed: 11056530]

Smith DS, Skene JH. A transcription-dependent switch controls competence of adult neurons for distinct modes of axon growth. J Neurosci Off J Soc Neurosci. 1997; 17:646–658.

Steiner P, Alberi S, Kulangara K, Yersin A, Sarria JC, Regulier E, Kasas S, Dietler G, Muller D, Catsicas S, Hirling H. Interactions between NEEP21, GRIP1 and GluR2 regulate sorting and recycling of the glutamate receptor subunit GluR2. EMBO J. 2005; 24:2873–2884. [PubMed: 16037816]

Talbot K, Cho D-S, Ong W-Y, Benson MA, Han L-Y, Kazi HA, Kamins J, Hahn C-G, Blake DJ, Arnold SE. Dysbindin-1 is a synaptic and microtubular protein that binds brain snapin. Hum Mol Genet. 2006; 15:3041–3054. DOI: 10.1093/hmg/ddl246 [PubMed: 16980328]

Taneichi-Kuroda S, Taya S, Hikita T, Fujino Y, Kaibuchi K. Direct interaction of Dysbindin with the AP-3 complex via its mu subunit. Neurochem Int. 2009; 54:431–438. DOI: 10.1016/j.neuint.2009.01.014 [PubMed: 19428785]

Taya S, Shinoda T, Tsuboi D, Asaki J, Nagai K, Hikita T, Kuroda S, Kuroda K, Shimizu M, Hirotsune S, Iwamatsu A, Kaibuchi K. DISC1 regulates the transport of the NUDEL/LIS1/14-3-3epsilon complex through kinesin-1. J Neurosci Off J Soc Neurosci. 2007; 27:15–26. DOI: 10.1523/JNEUROSCI.3826-06.2006

Vazdarjanova A, Bunting K, Muthusamy N, Bergson C. Calcyon upregulation in adolescence impairs response inhibition and working memory in adulthood. Mol Psychiatry. 2011; 16:672–684. DOI: 10.1038/mp.2011.14 [PubMed: 21403673]

Willemsen MH, Vissers LEL, Willemsen MAAP, van Bon BWM, Kroes T, de Ligt J, de Vries BB, Schoots J, Lugtenberg D, Hamel BCJ, van Bokhoven H, Brunner HG, Veltman JA, Kleefstra T. Mutations in DYNC1H1 cause severe intellectual disability with neuronal migration defects. J Med Genet. 2012; 49:179–183. DOI: 10.1136/jmedgenet-2011-100542 [PubMed: 22368300]

Xiao J, Dai R, Negyessy L, Bergson C. Calcyon, a novel partner of clathrin light chain, stimulates clathrin-mediated endocytosis. J Biol Chem. 2006; 281:15182–15193. [PubMed: 16595675]

Yamada M, Toba S, Yoshida Y, Haratani K, Mori D, Yano Y, Mimori-Kiyosue Y, Nakamura T, Itoh K, Fushiki S, Setou M, Wynshaw-Boris A, Torisawa T, Toyoshima YY, Hirotsune S. LIS1 and NDEL1 coordinate the plus-end-directed transport of cytoplasmic dynein. EMBO J. 2008; 27:2471–2483. DOI: 10.1038/emboj.2008.182 [PubMed: 18784752]

Yap CC, Winckler B. Harnessing the power of the endosome to regulate neural development. Neuron. 2012; 74:440–451. DOI: 10.1016/j.neuron.2012.04.015 [PubMed: 22578496]

Yap CC, Wisco D, Kujala P, Lasiecka ZM, Cannon JT, Chang MC, Hirling H, Klumperman J, Winckler B. The somatodendritic endosomal regulator NEEP21 facilitates axonal targeting of L1/NgCAM. JCell Biol. 2008; 180:827–842. [PubMed: 18299352]

Yin D-M, Chen Y-J, Liu S, Jiao H, Shen C, Sathyamurthy A, Lin TW, Xiong W-C, Li B-M, Mei L, Bergson C. Calcyon stimulates neuregulin 1 maturation and signaling. Mol Psychiatry. 2014; doi: 10.1038/mp.2014.131

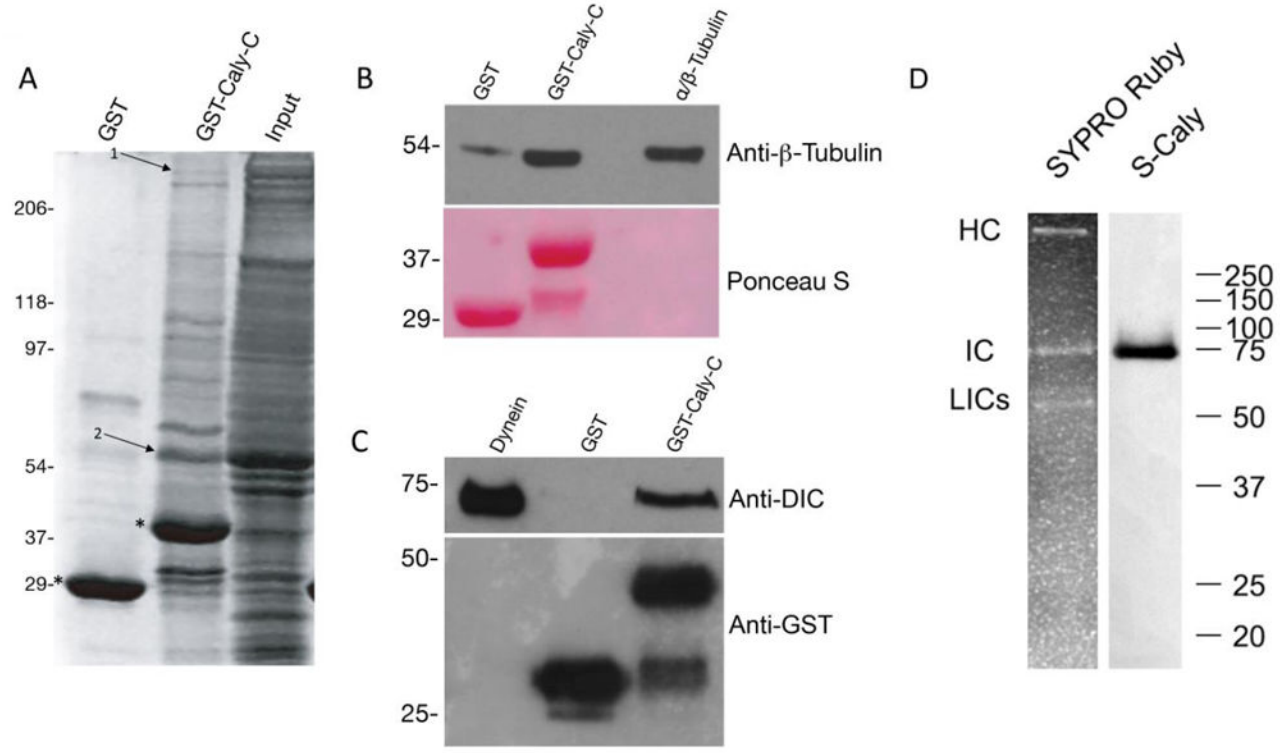

Figure 1. Association of brain microtubule proteins with Caly

A. SYPRO Ruby stained 1-D SDS gel of proteins eluted from resin-bound GST (left lane) or GST-Caly-C (middle lane) following incubation with homogenates of mouse forebrain (right lane). Numbered arrows point to two bands picked for trypsin digestion and subjected to MALDI-TOF MS that corresponded to microtubule related proteins. Asterisks show the position of the GST and GST-Caly-C bands in the GST and GST-Caly-C pull-down lanes, respectively. β tubulin (B) or DIC (C) antibody probing of immunoblots of proteins eluted from GST or GST-Caly following incubation with highly purified α/β tubulin or dynein complex, respectively. D. SYPRO Ruby stained PVDF membrane showing the subunits of purified dynein complex, including heavy chain (HC), intermediate chain (IC), and light intermediate chains (LICs). Purified S-protein tagged Caly-93-217 was incubated overnight with the membrane, and binding visualized with S-HRP. A single band corresponding to IC was detected by ECL.

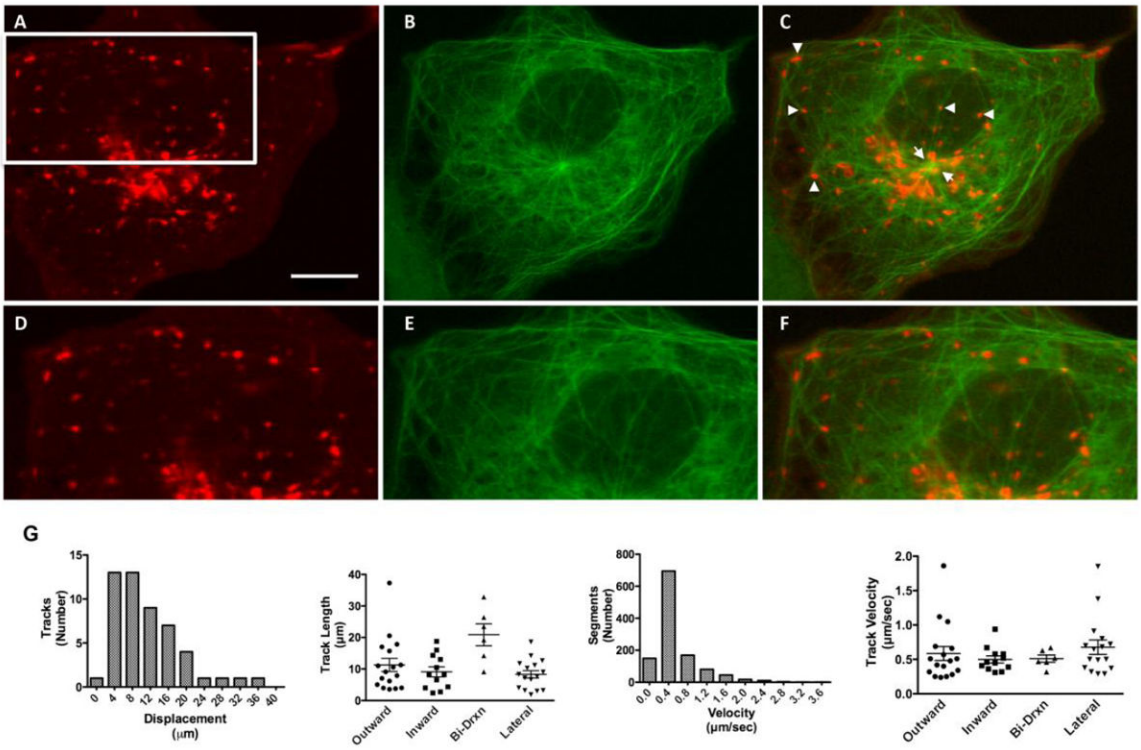

Figure 2. Localization and movement of Caly along the microtubule network

mCh-Caly (A,D) and GFP-tubulin (B,E) co-transfected Cos-7 cell. Region in solid boxed area in A is enlarged in panels D-F. (C,F) Arrowheads show Caly puncta arrayed along GFP-labeled microtubules in the merged images. Arrows point to concentration of mCh-Caly near the MTOC. Scale bar in A =10 μm. (G) Analyses of overall track or segment displacement, speed, and direction.

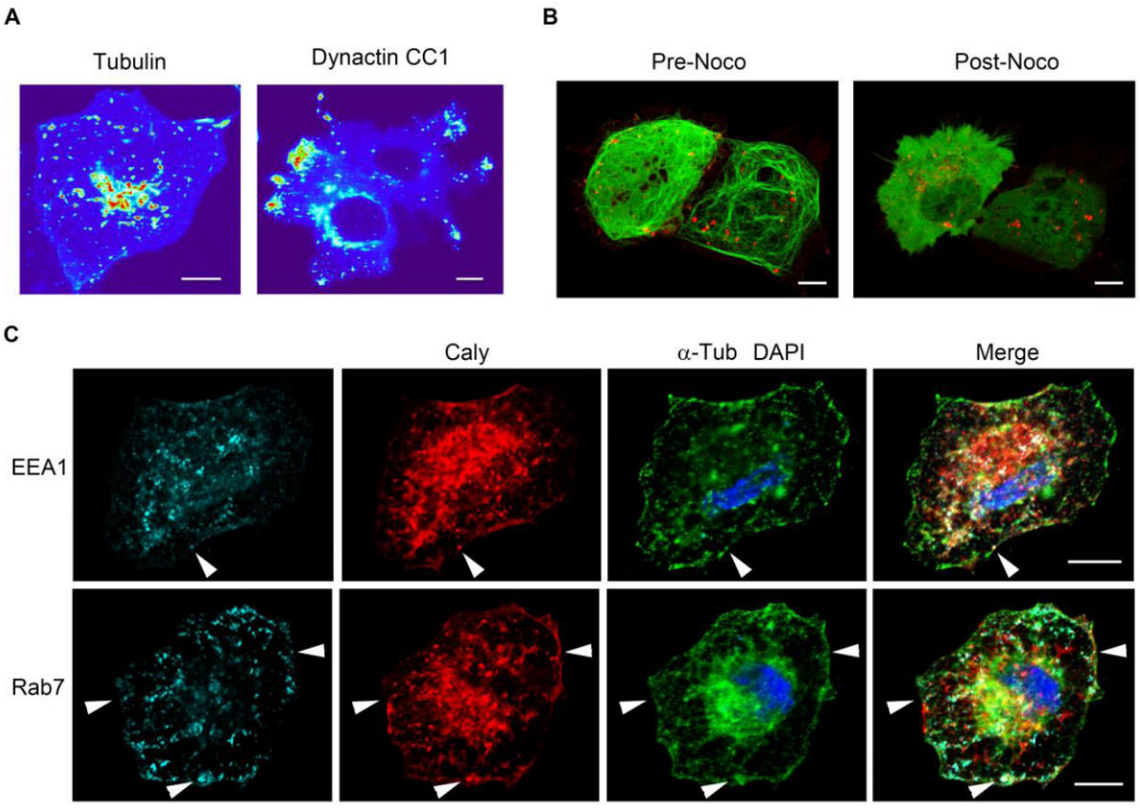

Figure 3. Dynein impacts Caly subcellular distribution and movement

A. Distribution of mCh-Caly in Cos-7 cells co-transfected with either tubulin, or the CC1 peptide of the dynactin p150 subunit, both expressed as GFP fusion proteins. B. Microtubule and Caly distribution in GFP-tubulin and mCh-Caly co-transfected cells before application of 10μM nocodazole (Pre-Noco) or after 80 min treatment (Post-Noco). Based on GFP-tubulin distribution, nocodazole disrupted microtubule structure, and also resulted in a cessation of Caly motility (Supplemental video 1,2). C. In fixed cells, Caly colocalized with early endosome (EEA1) and later endosome (Rab7), where α-tubulin stains tubulin polymers. Cells were also co-transfected with mCh-Caly and GFP-Rab5 or GFP-Rab7 to assess Caly motility in EEs and LEs, respectively (Supplemental video 3,4). Scale Bars =10 μm.

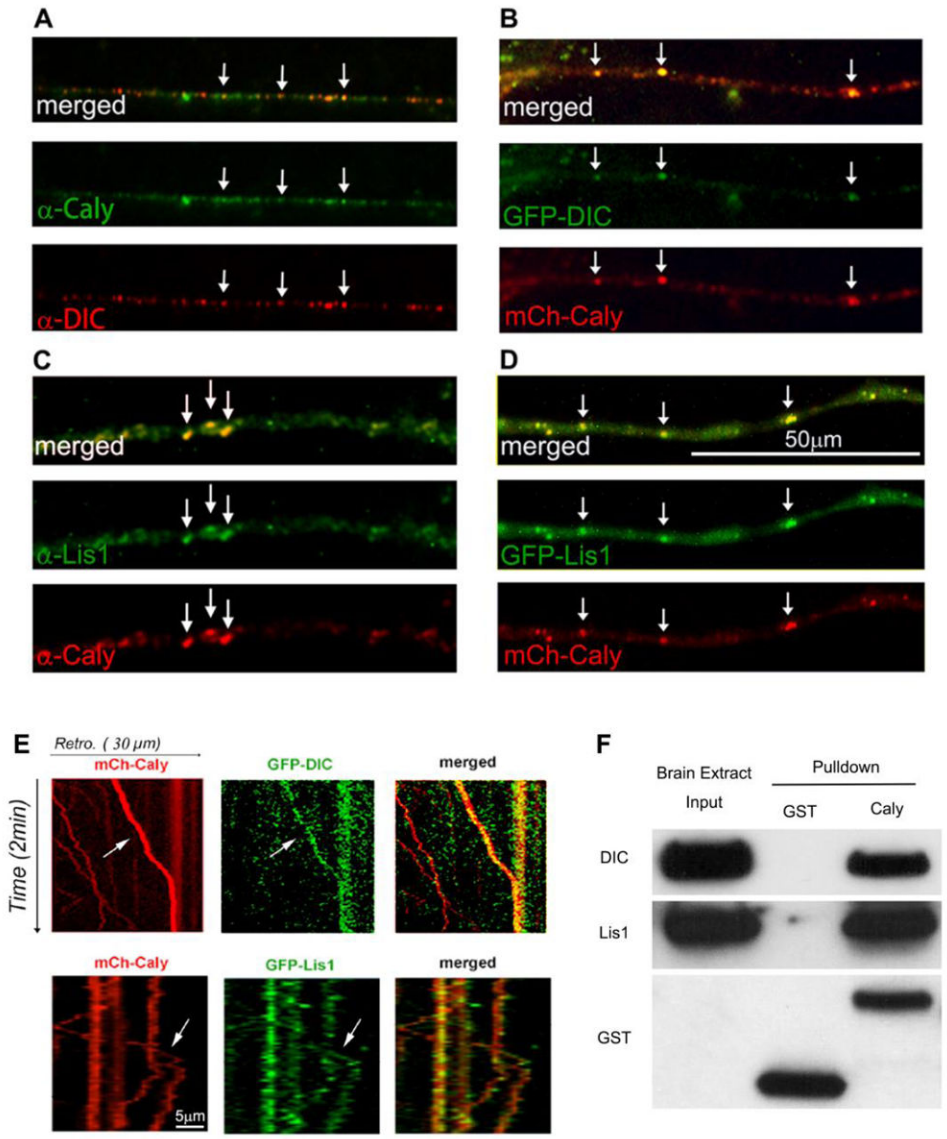

Figure 4. Complexes containing Caly and dynein are present in axons

Endogenous DIC (A) and Lis1 (C) co-localized with endogenous Caly puncta in axons extended by adult rat sensory neurons in culture (arrows). GFP-DIC (B) and GFP-Lis1 (D) co-localized with mCh-Caly puncta in DRG axons. Scale Bars=5 μm. (E) Time-lapse data from two-minute recordings of 30 μm axon segments were used to generate the kymographs of particles moving in DRG axons. GFP-DIC and GFP-Lis1 were observed moving with mCh-Caly in the same particle. F. Dynein and Lis1 were pulled down by GST-Caly from brain extracts. Equal amounts of GST and GST-Caly-C were incubated with brain extracts, eluted proteins were probed with anti-DIC, anti-Lis1 and anti-GST antibodies. Only GST-Caly showed the capacity to bind dynein and Lis1.

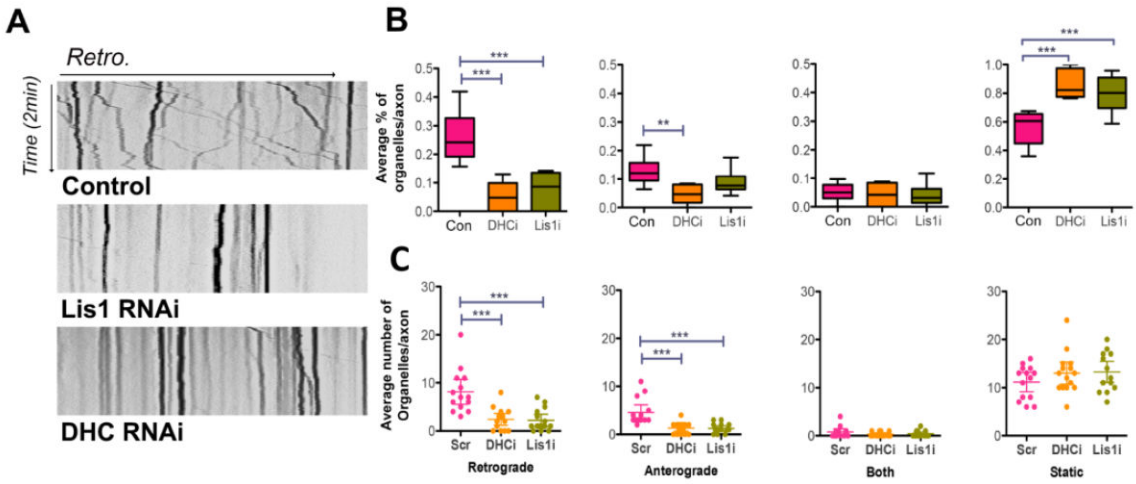

Figure 5. Dynein motors contribute to the motility of mCh-Caly organelles in DRG axons

(A) Representative kymographs of mCh-Caly organelles moving in axons of neurons expressing scrambled RNA (control), DHC RNAi, or Lis1 RNAi. (B, C) The percent (B) and numbers (C) of 4 classes of organelle movements were determined for 6-12 axons in three different experiments. Retrograde: towards the cell body; Anterograde: away from the cell body; Both: organelles switched directions one or more times; Static: organelles did not move during the recording interval. Total organelles examined: 346 (scr), 237 (DHC RNAi) and 256 (Lis1 RNAi). Significance determined by one-way ANOVA using Tukey's multiple comparisons post test; (B, C) *** $p<0.0001$; ** $p= 0.0051$.

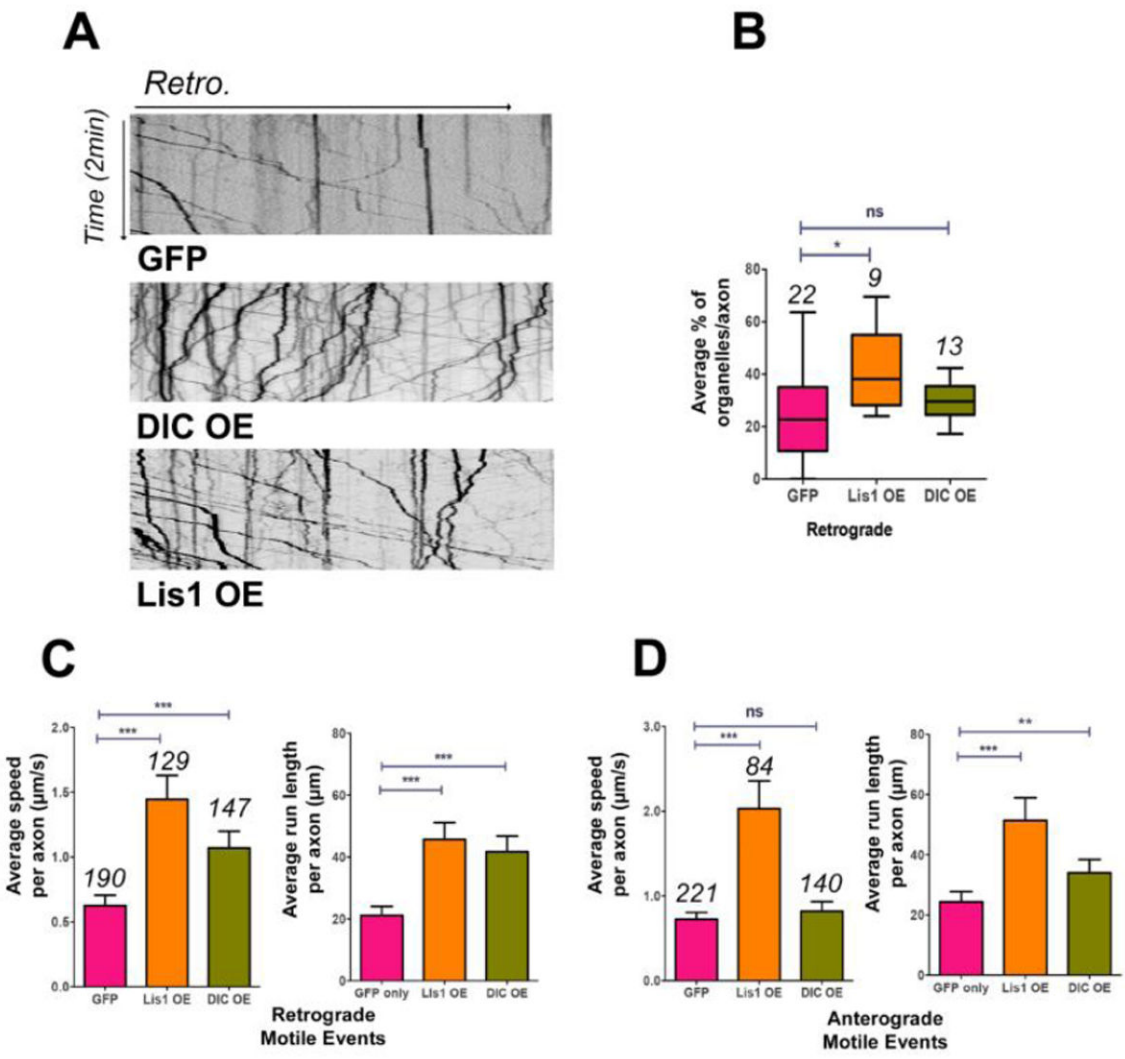

Figure 6. Lis1 and Dynein overexpression increases the motility of mCh-Caly organelles in DRG axons

(A) Kymographs of mCh-Caly organelles in axons overexpressing Lis1 and DIC. (B, C) Overexpression of Lis1 but not DIC increased the percentage of organelles classified as retrograde (numbers above bars is the number of axons analyzed for each condition). (D, E) Overexpression of Lis1 or DIC increased the speeds and run lengths of retrograde motile events. Lis1 increased the speed of anterograde motile events, and both Lis1 and DIC increased run lengths of anterograde motile events. (B) * $p<0.017$; (D,E) *** $p<0.0001$; ** $p=0.0007$.

Table 1

Results of MALDI-TOF Mass Spectrometric Analysis from Mus musculus databases

Protein Name	Accession No.	Protein MW	Peptide Count	Protein Score	% Cov
DYNEIN, CYTOPLASMIC, HEAVY CHAIN 1	gil13384736	534426.9	53	177	16.6
TUBULIN ALPHA-1A CHAIN	gil53733821	50803.9	9	165	27.5
TUBULIN ALPHA-1B CHAIN	gil34740335	50803.9	9	154	26.6
TUBULIN ALPHA-4A CHAIN, ISOFORM 1	gil6678467	50633.6	8	156	25.2
TUBULIN BETA-4B CHAIN	gil22165384	50255.2	11	150	28.1
SIMILAR TO TUBULIN BETA-2 CHAIN	gil51710798	50267.0	9	141	22.0
TUBB2A PROTEIN, PARTIAL	gil13097483	34207.5	10	129	33.6